

General Disclaimer

One or more of the Following Statements may affect this Document

- This document has been reproduced from the best copy furnished by the organizational source. It is being released in the interest of making available as much information as possible.
- This document may contain data, which exceeds the sheet parameters. It was furnished in this condition by the organizational source and is the best copy available.
- This document may contain tone-on-tone or color graphs, charts and/or pictures, which have been reproduced in black and white.
- This document is paginated as submitted by the original source.
- Portions of this document are not fully legible due to the historical nature of some of the material. However, it is the best reproduction available from the original submission.

NASA Technical Memorandum 82776
AIAA-82-0192

08651
Riddle
Stack

(NASA-TM-82776) DILUTION JET BEHAVIOR IN
THE TURN SECTION OF A REVERSE FLOW COMBUSTER
(NASA) 15 p HC A02/MF A01 CSDL 21E

N82-19220

Unclass

G3/07 08956

Dilution Jet Behavior in the Turn Section of a Reverse Flow Combuster

Steven M. Riddlebaugh
*Lewis Research Center
Cleveland, Ohio*

and

Abraham Lipshitz
Ahuza, Haifa, Israel

and

Isaac Greber
*Case Western Reserve University
Cleveland, Ohio*



Prepared for the
Twentieth Aerospace Sciences Meeting
sponsored by the American Institute of Aeronautics
and Astronautics
Orlando, Florida, January 10-14, 1982

NASA

DILUTION JET BEHAVIOR IN THE TURN SECTION
OF A REVERSE FLOW COMBUSTOR

by Stephen M. Riddlebaugh
National Aeronautics and Space Administration
Lewis Research Center
Cleveland, Ohio 44135

and

Abraham Lipshitz
58 Horev Street
Ahuz, Haifa, 34343, Israel

and

Isaac Greber*
Case Western Reserve University
Cleveland, Ohio 44106

Abstract

Measurements of the temperature field produced by a single jet and a row of dilution jets issued into a reverse flow combustor are presented. The temperature measurements are presented in the form of consecutive normalized temperature profiles, and jet trajectories. Single jet trajectories were swept toward the inner wall of the turn, whether injection was from the inner or outer wall. This behavior is explained by the radially inward velocity component necessary to support irrotational flow through the turn. Comparison between experimental results and model calculations showed poor agreement due to the model's not including the radial velocity component. A widely spaced row of jets produced trajectories similar to single jets at similar test conditions, but as spacing ratio was reduced, penetration was reduced to the point where the dilution jet flow attached to the wall.

Introduction

The reverse flow combustor for gas turbine engines derives its name from the fact that the gas flow direction in the combustor is opposite to the overall gas flow direction through the engine. Thus, the combustion gases must be turned up to 180° before entering the turbine. A cutaway drawing of a full scale research reverse flow combustor is shown in Fig. 1.

The reverse flow configuration has certain characteristics that make it an attractive design for small turboshaft engines where its large annulus diameter does not incur a drag penalty. These engines often have a centrifugal high pressure compressor and the reverse flow combustor is easily coupled to this compressor.

This combustor type has a number of design challenges, many of which are associated with the region where the combustion gases are turned. This region, or turn section, may also be the region where the dilution air is mixed with the combustion gases to produce the desired temperature profile at the combustor exit.

One major problem is the determination of dilution jet behavior in an accelerating and turning flow field such as is found in the turn section of the reverse flow combustor. The trend in gas turbine engine cycles is ever higher turbine inlet temperatures, and as materials and design limits of turbine blades are approached it becomes increasingly more important to precisely tailor the combustor exit temperature profile. Since a significant part of this tailoring is done by the dilution air there is an increasing need for a better understanding of the dilution jet mixing phenomena associated with this combustor type.

A recently completed research program conducted by Case Western Reserve University under a NASA grant (NSG 3206) studied and modeled the behavior of dilution jets entering on accelerating and turning flow field. The early phases of this program involved tests of two dimensional water flow models of the turn section, and development of a mathematical model. The results of this phase were reported in Ref. 2.

In order to gain insight into applying this model to a reverse flow combustor situation, and to provide a data base for future refinement of the model, a small reverse flow combustor sector was designed, fabricated and tested. The combustor was designed such that the gas temperatures throughout the turn section could be mapped. The dilution zone was represented by multiple rows of entry ports that could be capped or connected to a controlled air supply such that axial locations of the dilution jets, and their spacing geometries could be varied.

The combustor was operated over a range of conditions in which the density ratios and momentum ratios of the dilution jet to the combustion gases were varied. The temperature data were stored in a computer for future access. The measured temperature patterns were compared to the model predictions.

Apparatus and Test Procedure

A cutaway sketch of the test combustor is shown in Fig. 2. Figure 3 is a photograph of the test combustor. The overall size and geometry roughly duplicated the full annular research combustor shown in Fig. 1. Due to a flow rate limitation and exhaust considerations the test

*Chairman, Dept. of Mechanical and Aerospace Engineering.

combustor was a 90° sector of a full circle. The aspect ratio to the primary zone (before the turn) was 7.25 and at the exit was 7.8, believed to be large enough to approximate a two dimensional flow behavior in the central region of the sector without significant sidewall effects.

The combustor was a low pressure, uncooled design burning low pressure natural gas in eight tunnel burners located 43 cm upstream of the turn. Each burner was fed a near stoichiometric, slightly rich premixed air-natural gas mixture and was encircled by a series of small holes admitting primary zone cooling air.

The primary zone of the combustor was made of Inconel-750 X alloy, allowing a wall temperature of up to 920 K (1200° F) without significant warpage. The walls of the turn section were type 304 stainless steel.

The dilution jet entry ports were a series of pipe nipples brazed to the combustor. Dilution jet entry geometry was varied by connecting the appropriate nipples and capping the unused ones. Due to space limitations it was possible to install a row of dilution jet entries at only one axial location on the inner wall (injection point A in Fig. 4). On the outer wall rows of dilution jet entries were fitted at two axial locations, points B and C. Points A and B were located 5.1 cm upstream of the start of the turn, while point C was located 14° into the turn.

The dilution jet entry holes were 7.11 mm in diameter, the size being dictated by the fittings used. Each row of jets consisted of 21 entry holes; because of the geometry of the test section the spacing ratios (S/D) of the ID, OD, and in-the-bend rows were different. Injection point A had a spacing ratio of 2.47. Injection point B had an S/D of 3.07, while point C had an S/D of 3.06. The ratio of the duct height to injection hole diameter (H/D) was 8.02 for injection locations A and B, and 8.03 for location C.

The inner and outer walls of the turn section were circular in profile, with radii of 3.6 and 8.1 cm, respectively. In order to produce a converging duct the centers of the two radii were offset 1.3 cm. Duct height ranged from 5.7 cm at the beginning of the turn to 3.3 cm at the combustor exit.

This geometry was chosen for two reasons. The first was that this greatly simplified fabrication; the toroidal pieces were made by splitting standard pipe elbows lengthwise. The second reason was that this allowed the fitting of a moveable thermocouple rake that could rotate through the turn section as well as make radial traverses. The position of this rake was controlled by two hand cranks.

The air supply was a centrifugal blower providing 7 kilopascals (1 psig) pressure at about 1 kg/s (2 lb/sec) flow rate. The fuel was low pressure commercial natural gas. Air and natural gas flow rates were monitored by standard orifice runs connected to manometer tubes or pressure gauges.

Apart from pressure taps in the air and natural gas supply lines, instrumentation consisted of thermocouples mounted on the combustor walls for

rig monitoring and in the primary zone main gas stream and dilution air supply manifolding for research data measurements. Dilution air temperature was measured by thermocouples inserted into the manifolding system, including a probe inserted in the supply line about 2 cm upstream of the point of injection into the combustor.

Figure 4 shows the research instrumentation in the turn section of the combustor. There were 10 measuring stations spaced 20 degrees apart. The temperature rake, which was traversed radially, contained five thermocouples arranged horizontally such that five parallel "layers" of data were mapped, producing a three dimensional map of the turn section that was about 5 cm thick. Due to the 13 mm offset of the probe tips from the shaft of the rake the traverse paths at each measuring station were not quite radial in direction. Station 1 was immediately upstream of the start of the turn while station 10 was just upstream of the combustor exit. Temperature measurements were made at 9 radial locations at stations 1 to 5; 8 radial points at station 6; 7 points at station 7; and so on to 4 radial points at station 10. Thus, each test point condition a 3 dimensional array of 375 temperature measurements mapping the turn section.

Figure 5 is a photograph of the test installation. The test combustor is mounted vertically in the foreground. The combustor exhausted into an atmospheric dump. The thermocouple signals were processed by a digital thermometer and stored on a computer disk.

Each set of experiments consisted of a single dilution jet geometry operated at a range of momentum ratios and density ratios. This was done by varying the combustion gas temperature and combustion and dilution system flow rates. The combustion gas temperature at the exit of the primary zone was varied between 650 K (710° F) to about 820 K (1020° F). The dilution jet temperature was about 300 K (80° F). The combustor reference velocity was varied from about 8 to 12 m/sec (24 to 36 ft/sec) and the dilution jet injection velocity was varied from 10 to 25 m/sec (30 to 75 ft/sec).

Test conditions consisted of three or more momentum ratios ranging from 5.7 to about 11, at each of the two density ratios of about 2.14 and 2.74.

Results and Discussion

A three dimensional array of temperature measurements covering a central band of the turn section of a 90° sector reverse flow combustor were recorded for a variety of dilution jet entry geometries, momentum ratios, and density ratios.

The temperature data are presented in terms of a nondimensionalized parameter θ :

$$\theta = \frac{T_s - T}{T_s - T_j}$$

where:

T_s average primary zone gas temperature
 upstream of the dilution jet entry
 T local temperature
 T_j dilution jet air temperature just before
 injection into the combustor.

The centerlines of the dilution jet trajectories are also presented. The locations of the trajectories were identified as the coldest point (largest θ) in the temperature profile at each measuring station.

Figure 6 shows the temperature distribution in the combustor turn without dilution jets. This "base line" distribution showed a definite radial profile at the initial stations; the gas temperatures close to the inner wall were noticeably lower than the average temperature (corresponding to $\theta = 0$). This overly thick boundary layer effect was apparently a combination of burner performance and imperfect mating of combustor sections. By station 5 the radial profile was flattened out, partly a consequence of the converging walls. The temperature distortion at station 1, the worst case, corresponded to a pattern factor of 0.17.

Single Jet Results

Figure 7 shows the temperature distribution for a single jet injected from the inner wall (point A in Fig. 4). The centerline of the jet penetrated to about the centerline of the combustor annulus and then drifted back toward the inner wall of the turn. Beyond station 4 the profiles were too flat to locate a definite path, although the profiles suggest a drift toward the inner wall of the turn.

This sweeping of the jets toward the inner wall of the turn was a surprising behavior. It was expected that the dilution jets, being cooler and thus denser than the combustion gases, would migrate toward the outer wall of the turn, as was the case in the preliminary 2D testing with water.²

This inward drift may be explained in the following manner.³ From an essentially uniform velocity profile upstream of the turn, the combustion gases accelerate along the inner wall relative to the outer wall as they negotiate the turn. Conservation of mass requires an inward velocity component to support this developing skewed distribution. The corresponding combination of increased radial pressure gradient and increased normal velocity of the combustion gases with respect to the jet are sufficient to drive the jet inward.

Figure 8 shows the temperature distribution for a single jet injected from the outer wall (point B in Fig. 4). As in the case with the jet injected from the inner wall, the centerline of the jet tended to drift toward the inner wall in the bend. In both cases there was considerable mixing of the jet and main stream by station 5, as indicated by a flat temperature profile.

When the jet injection point was moved downstream into the outer wall of the turn (point C in Fig. 4), behavior of the jet in terms of path and mixing were not appreciably altered from the previous case, except for being shifted downstream a

distance roughly corresponding to the shift in injection point.

The next two figures present the effects of increasing the momentum ratio of the dilution jet with respect to the mainstream. Figure 9 shows the effect of the momentum ratio on a jet injected from the inner wall. Increasing the momentum ratio resulted in greater penetration of the jet. Figure 10 shows the effect of momentum ratio on a jet injected from the outer wall. Again, increasing the momentum ratio increased jet penetration. For a momentum ratio of 9.61 the jet penetrated to the inner wall. Moving the injection point downstream into the turn simply shifted the pattern downstream with little change in effect.

Figures 11 and 12 present the effect of varying the density ratio of the dilution jet with respect to the mainstream at constant momentum ratios. In all cases the denser fluid penetrated farther into the main stream but the increase in penetration was greater for the jet being injected from the inner wall (Fig. 11) than for the jet being injected from the outer wall (Fig. 12). This is probably due to centrifugal forces acting on the denser fluid as it moves through the turn. In the outer-wall-injected cases the deeper penetration of the denser jet is partially cancelled by the centrifugal forces.

Multiple Jet Results

Figures 13 to 16 present the behavior of various configurations of rows of dilution jets, compared to single jet performance at the same test condition. In order to match momentum ratios, the single jet trajectories were interpolated from the data presented in Figs. 9 and 10. The profile plots as presented in Figs. 7 and 8 show typical behavior of the single jet situation, but the difference in momentum ratios between the single jet and multiple jet data should be taken into account when comparing the two sets of figures.

In all cases involving multiple jets (Figs. 13 to 16) penetration of the row of jets was less than that of the single jet. As the spacing ratio (distance between hole centerlines compared to hole diameter) increased, the performance of the row of jets approached the single jet. When the jets were closely spaced penetration was greatly reduced. In the case where the closely spaced jets were injected from the inner wall (Fig. 14) there was the extreme situation of practically no penetration into the main flow; the dilution jets in effect behaved like a film cooling slot.

When the closely spaced jets were injected from the outer wall (Fig. 16) initial penetration was roughly half the single jet case, but then the centerline of the jet moved toward the outer wall rather than drift toward the inner wall of the turn. In this region of the turn centrifugal forces on the denser jet apparently overcame the inward drift effect and drove the jet radially outward.

It is apparent that a model based on single jet data will not accurately predict the behavior of a row of jets except for fairly large spacing ratios. The results of this test suggest a spacing ratio of greater than 10 would produce single jet behavior for the test combustor.

A single jet injected into a cross flow approaches the classic situation of flow around a cylinder, which is the starting point of most models of this flow phenomena.^{2,3} For a row of jets with wide enough spacing between jets the flow field around each jet reaches the "infinity" condition between the jets. As the spacing decreases the flow fields around adjacent jets begin to interfere with each other. The overall drag of the row of jets increases and their trajectories are driven closer to the wall.

Comparison with Model

The initial part of this program, reported in Ref. 3, included derivation of a model based on two dimensional water flow tests. Figures 17 and 18 compare actual performance of a single dilution jet in the combustor with performance predicted by this model. In all cases the model predicted that the jet trajectory would migrate to the outer wall of the turn, whereas in the actual tests the jet trajectory migrated toward the inner wall of the turn. The model assumed that the centrifugal forces on the denser fluid in the jet would drive it outward as it was accelerated around the turn. In the tests the inward drift required to conserve mass³ apparently cancelled the centrifugal effect except in cases where the initial penetration carried the jet close to the outer wall of the turn.

Conclusion

1. In the turn section of the reverse flow combustor there was an inward transverse velocity component due to the developing nature of the flow. This effect and its associated pressure gradients were found to be very important in forming the dilution jet trajectory. As a consequence the main flow velocity field must be well known and accurately described for a model to accurately predict the behavior of a single jet or row of jets in the dilution zone.

2. A row of widely spaced jets produced a penetration trajectory similar to the pattern axially downstream of a single jet. An analytical model based on single jet data should make a reasonably accurate prediction of the behavior of a row of jets, provided the spacing ratio is sufficiently high (about 10 for the combustor geometry and hole size tested).

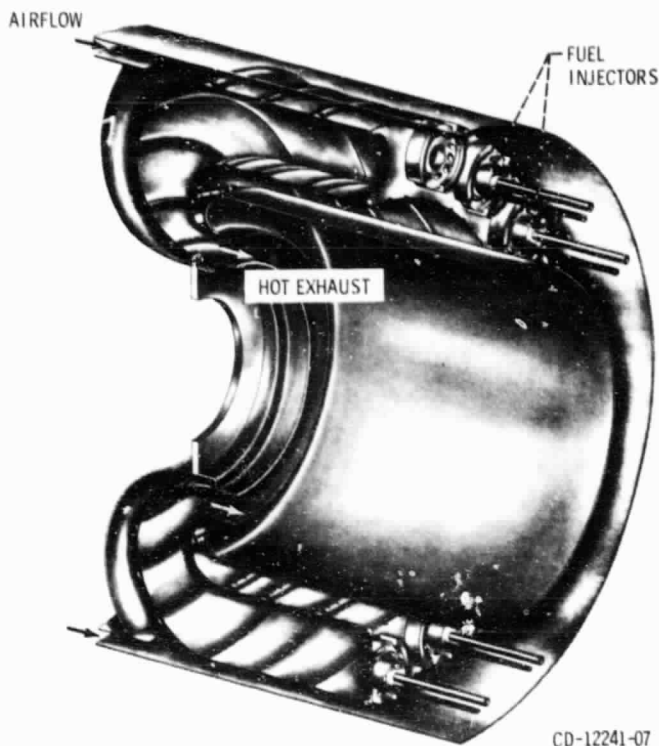
3. A row of closely spaced jets performed altogether differently than a single jet. As spacing between jets decreased, jet penetration decreased, due to the flow fields around each jet interfering with each other and increasing resistance to the main flow. In this test, spacing ratios of about 3 resulted in the dilution jets not penetrating the main stream.

4. Shifting the outer wall dilution jet penetration point downstream into the turn did not significantly change the jet penetration pattern other than move it downstream.

References

1. Demetri, E. P., Topping, R. F., and Wilson, R. P., Jr., "Study of Research and Development Requirements of Small Gas-Turbine Combustors," Arthur D. Little, Inc., Cambridge, Mass., ADL 83381-2, Jan. 1980. (NASA CR-159796)
2. Lipshitz, A. and Greber, I., "Turbulent Jet Patterns in Accelerating Flows," AIAA Paper 81-0348, 1981.
3. Lipshitz, A., "Dilution Jets in Accelerated Cross Flows," Ph.D. Thesis, Case Western Reserve University, May 1981.

ORIGINAL PAGE
BLACK AND WHITE PHOTOGRAPH



CD-12241-07

Figure 1. - Reverse flow combustor.

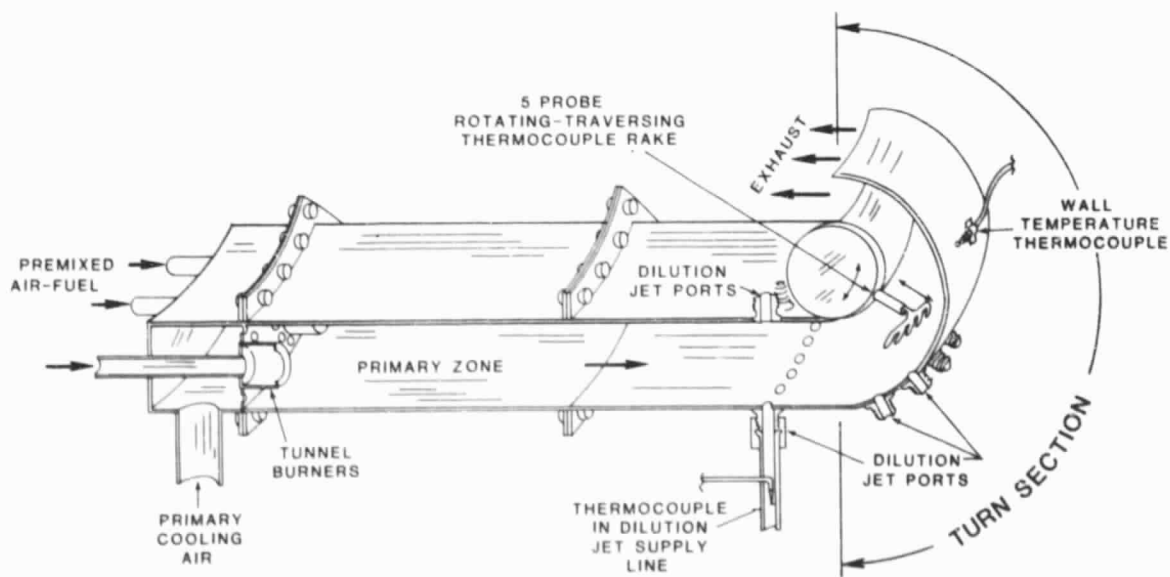


FIGURE 2. CUTAWAY SKETCH OF TEST COMBUSTOR

ORIGINAL PAGE
BLACK AND WHITE PHOTOGRAPH

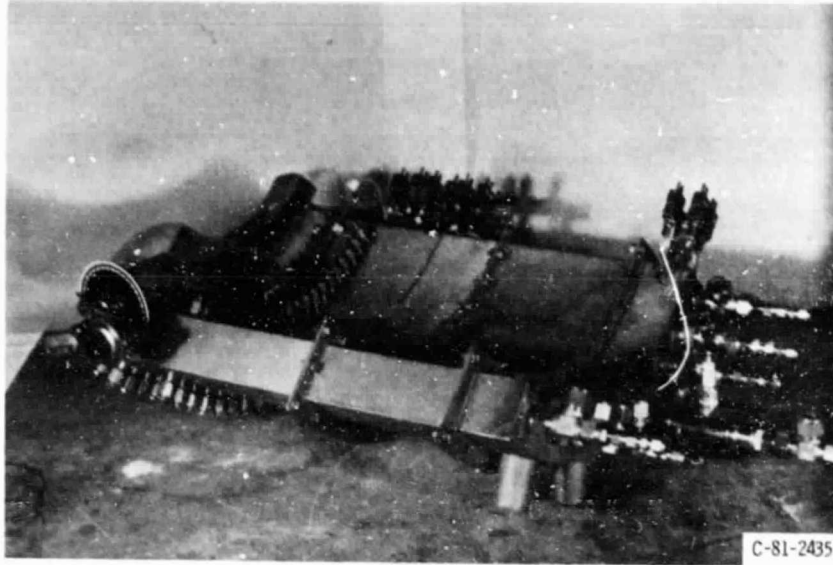


Figure 3. - Test section.

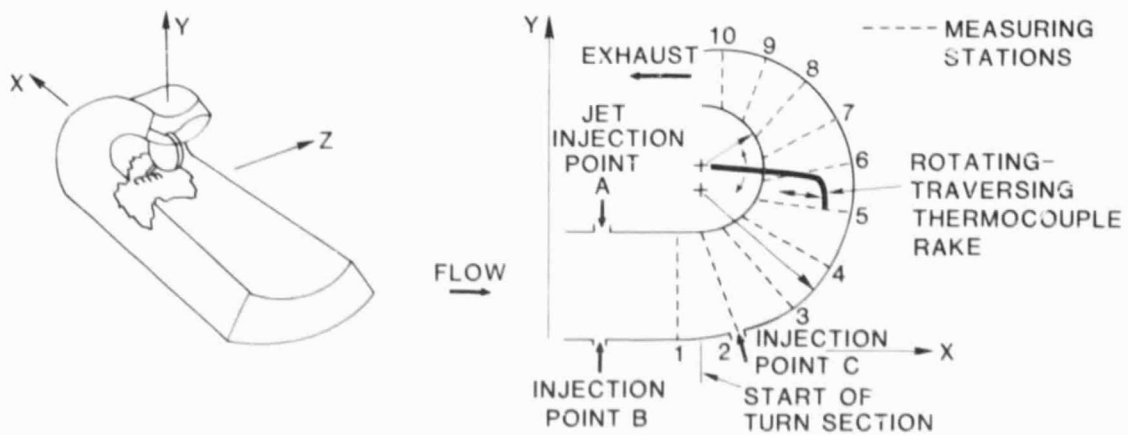


FIGURE 4. COMBUSTOR TURN SECTION GEOMETRY
AND TEMPERATURE MEASURING STATIONS

ORIGINAL PAGE
BLACK AND WHITE PHOTOGRAPH



Figure 5. - Test installation.

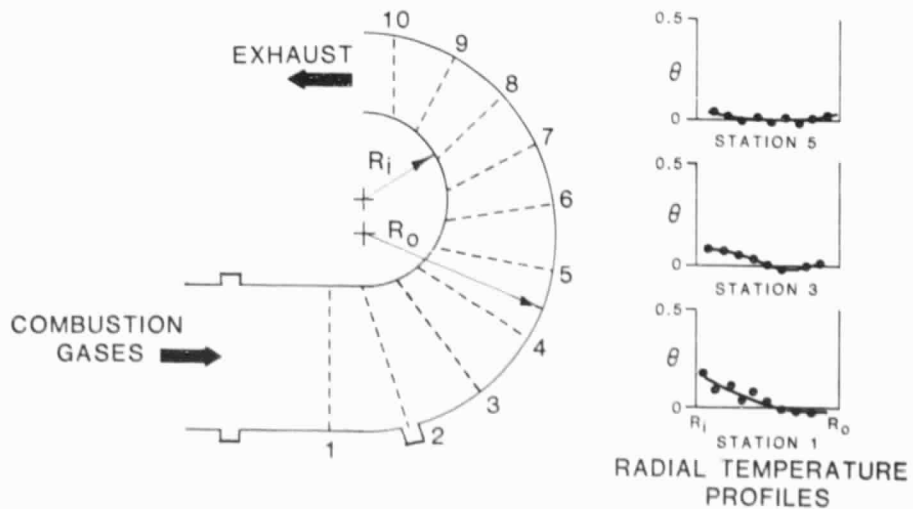
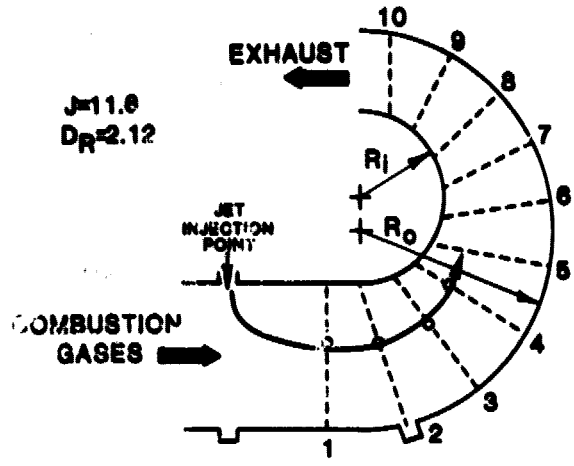


FIGURE 6. TEMPERATURE DISTRIBUTION IN THE COMBUSTOR
TURN WITHOUT DILUTION JETS



$J=11.6$
 $D_R=2.12$

COMBUSTION GASES

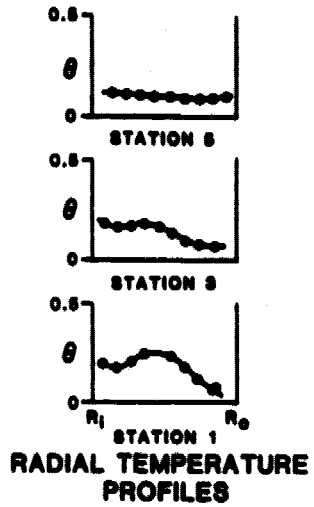
EXHAUST

JET INJECTION POINT

R_i

R_o

JET CENTERLINE TRAJECTORY



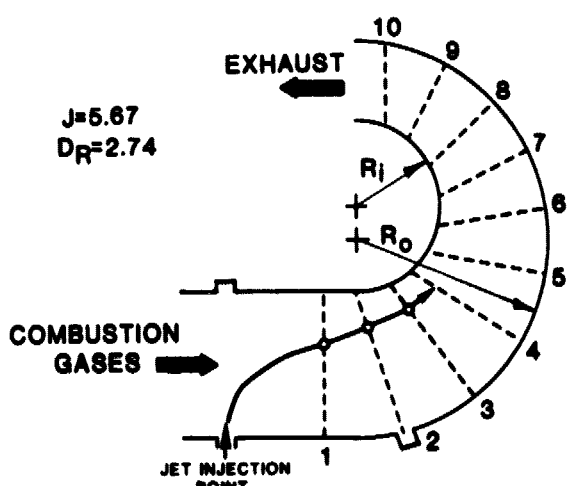
STATION 5

STATION 3

STATION 1

RADIAL TEMPERATURE PROFILES

FIGURE 7. TEMPERATURE DISTRIBUTION FOR A JET INJECTED FROM THE INNER WALL



$J=5.67$
 $D_R=2.74$

COMBUSTION GASES

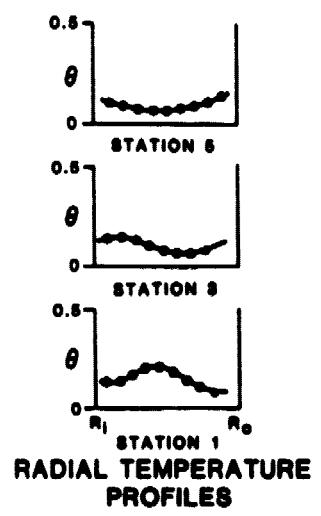
EXHAUST

JET INJECTION POINT

R_i

R_o

JET CENTERLINE TRAJECTORY



STATION 5

STATION 3

STATION 1

RADIAL TEMPERATURE PROFILES

FIGURE 8. TEMPERATURE DISTRIBUTION FOR A SINGLE JET INJECTED FROM THE OUTER WALL

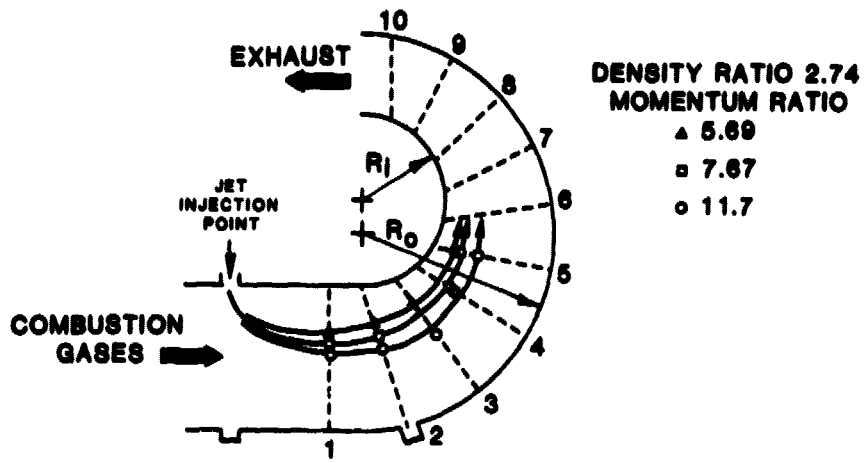


FIGURE 9. JET TRAJECTORIES SHOWING EFFECT OF MOMENTUM RATIO ON A JET INJECTED FROM THE INNER WALL

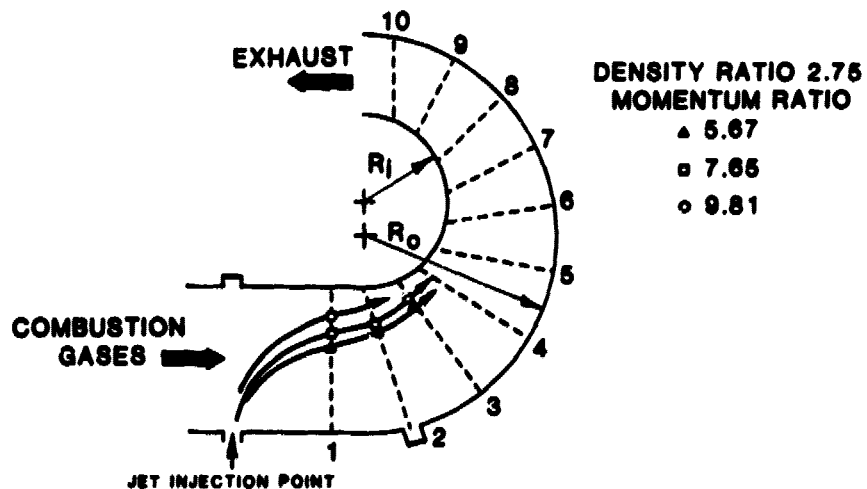


FIGURE 10. JET TRAJECTORIES SHOWING EFFECT OF MOMENTUM RATIO ON JET INJECTED FROM THE OUTER WALL

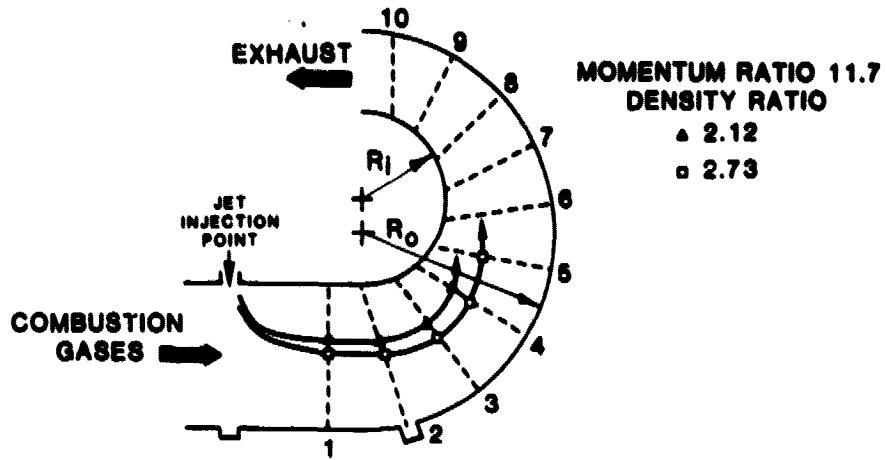


FIGURE 11. JET TRAJECTORIES SHOWING EFFECT OF DENSITY RATIO ON A JET INJECTED FROM THE INNER WALL

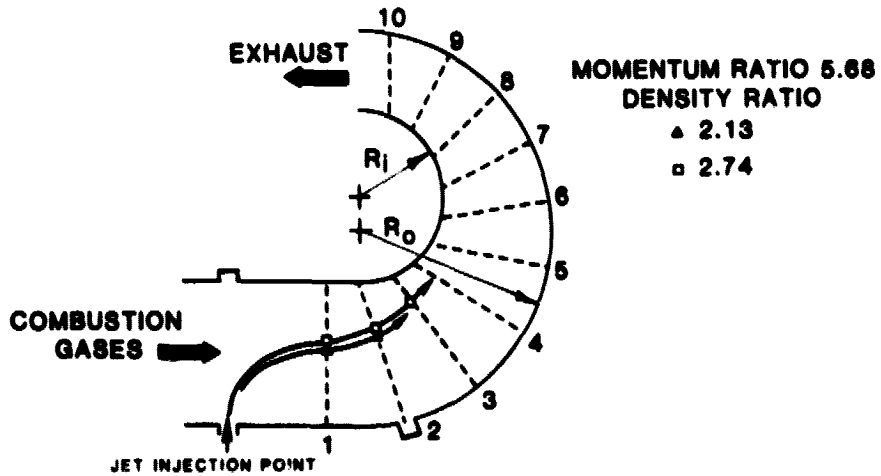


FIGURE 12. JET TRAJECTORIES SHOWING EFFECT OF DENSITY RATIO ON A JET INJECTED FROM THE OUTER WALL

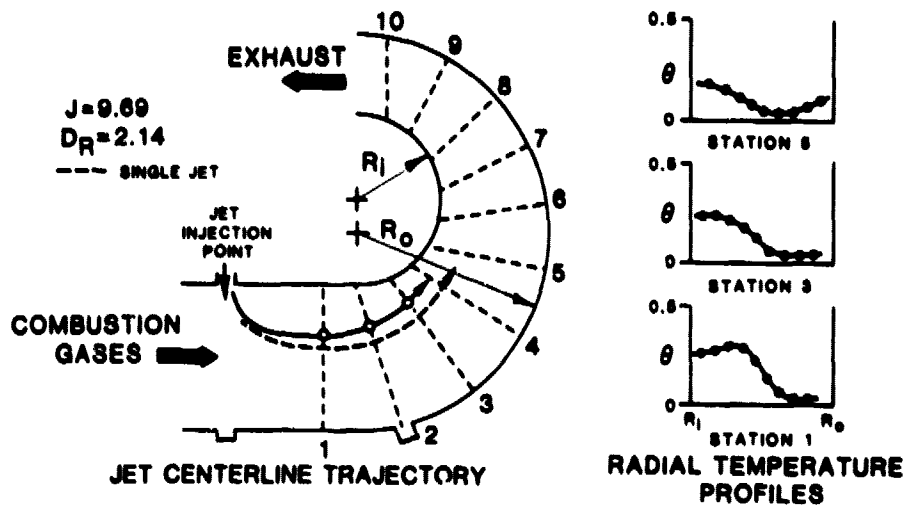


FIGURE 13. BEHAVIOR OF A WIDELY SPACED ROW OF JETS (SPACING RATIO OF 7.41) INJECTED FROM THE INSIDE WALL

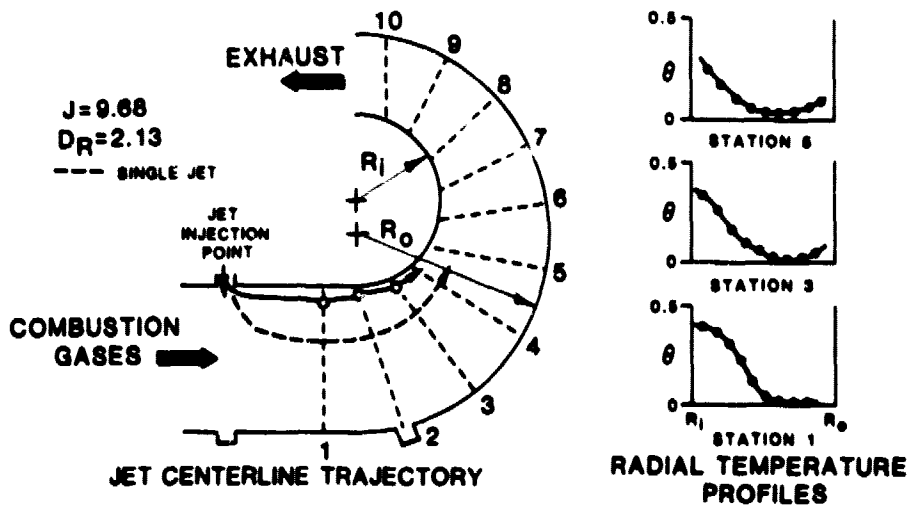


FIGURE 14. BEHAVIOR OF A CLOSELY SPACED ROW OF JETS (SPACING RATIO 2.47) INJECTED FROM THE INSIDE WALL

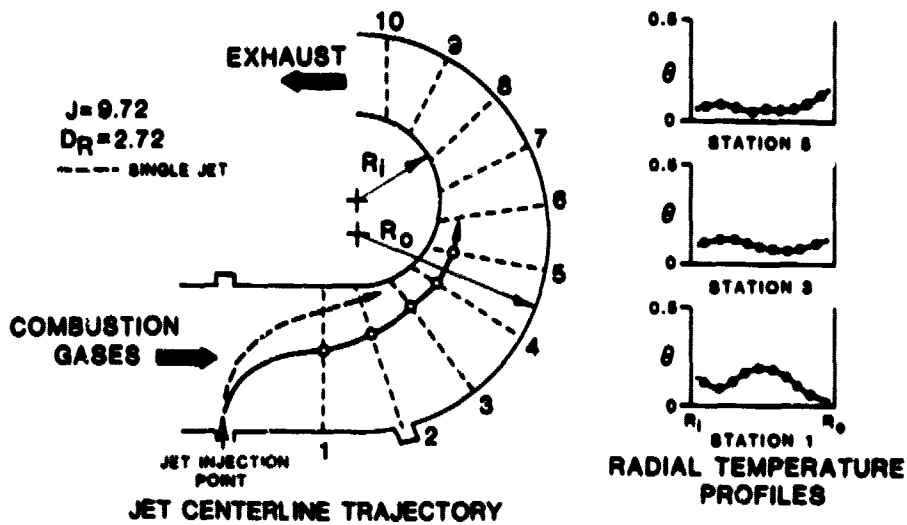


FIGURE 15. BEHAVIOR OF A WIDELY SPACED ROW OF JETS (SPACING RATIO 9.21) INJECTED FROM THE OUTSIDE WALL

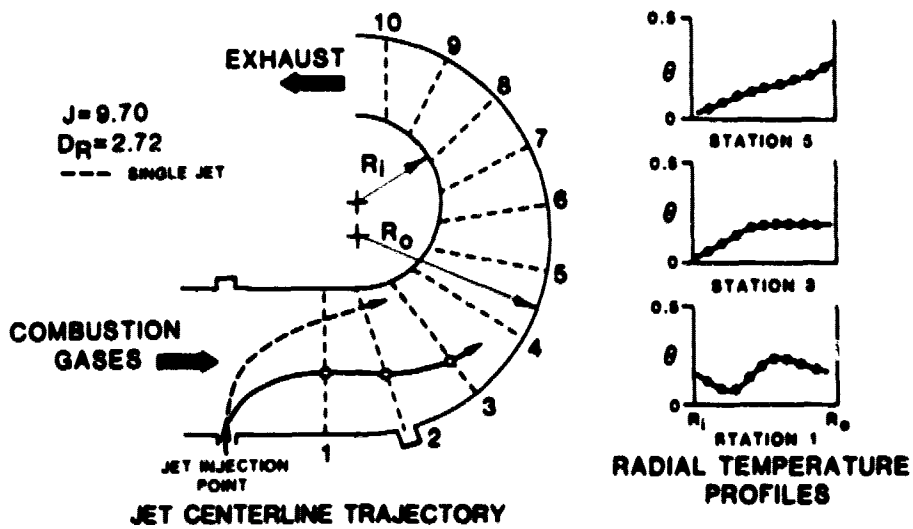


FIGURE 16. BEHAVIOR OF A CLOSELY SPACED ROW OF JETS (SPACING RATIO 3.07) INJECTED FROM THE OUTSIDE WALL

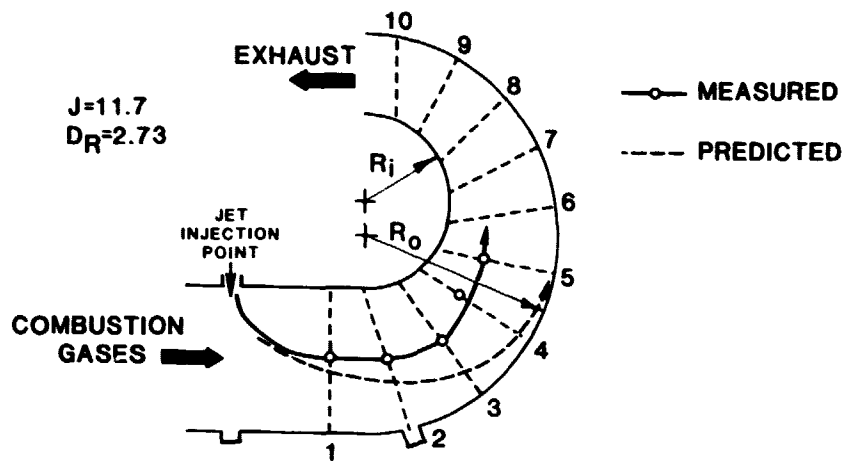


FIGURE 17. COMPARISON WITH MODEL FOR A SINGLE JET INJECTED FROM THE INNER WALL

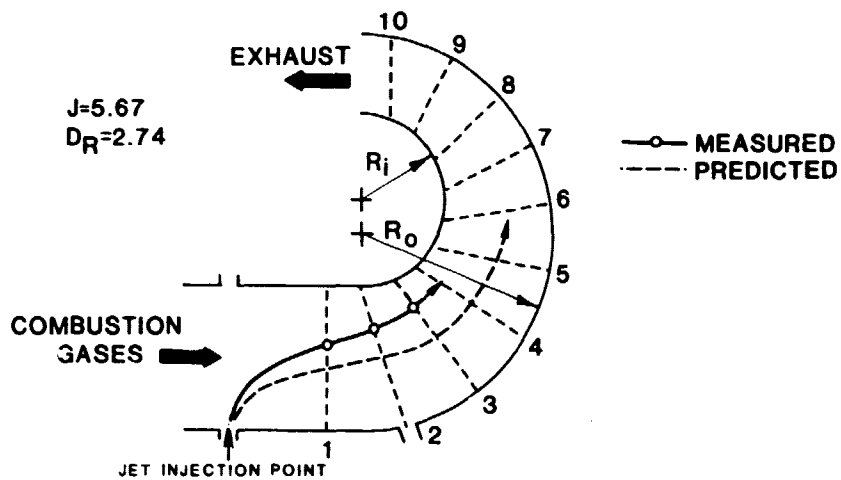


FIGURE 18. COMPARISON WITH MODEL FOR A SINGLE JET INJECTED FROM THE OUTER WALL